

# The Extended Bose-Hubbard Model on a Honeycomb Lattice

Jing Yu Gan,<sup>1</sup> Yu Chuan Wen,<sup>2,3</sup> Jinwu Ye,<sup>4</sup> Tao Li,<sup>5</sup> Shi-Jie Yang,<sup>6</sup> and Yue Yu<sup>3</sup>

<sup>1</sup>Center for Advanced Study, Tsinghua University, Beijing, 100084, China

<sup>2</sup>Interdisciplinary Center of Theoretical Studies, CAS, Beijing 100080, China

<sup>3</sup>Institute of Theoretical Physics, CAS, Beijing 100080, China

<sup>4</sup>Department of Physics, The Pennsylvania State University, University Park, PA, 16802, U.S.A.

<sup>5</sup>Department of Physics, Renmin University of China, Beijing 100872, China

<sup>6</sup>Department of Physics, Beijing Normal University, Beijing 100875, China

We study the extended Bose-Hubbard model on a two-dimensional honeycomb lattice by using large scale quantum Monte Carlo simulations. We present the ground state phase diagrams for both the hard-core case and the soft-core case. For the hard-core case, the transition between  $\rho = 1/2$  solid and the superfluid is first order and the supersolid state is unstable towards phase separation. For the soft-core case, due to the presence of the multiple occupation, a stable particle induced supersolid (SS-p) phase emerges when  $1/2 < \rho < 1$ . The transition from the solid at  $\rho = 1/2$  to the SS-p is second order with the superfluid density scaling as  $\rho_s \sim \rho - 1/2$ . The SS-p has the same diagonal order as the solid at  $\rho = 1/2$ . As the chemical potential increasing further, the SS-p will turn into a solid where two bosons occupying each site of a sublattice through a first order transition. We also calculate the critical exponents of the transition between  $\rho = 1/2$  solid and superfluid at the Heisenberg point for the hard core case. We find the dynamical critical exponent  $z = 0.15$ , which is smaller than results obtained on smaller lattices. This indicates that  $z$  approaches zero in the thermodynamic limit, so the transition is also first order even at the Heisenberg point.

Bose-Hubbard model and its derivatives have been extensively studied as the low energy effective models for ultracold atoms in optical lattices where the superfluid to the Mott insulator transition exists in the zero temperature [1, 2, 3], as well as models for the possible supersolid phases in both bipartite and frustrated lattices [4, 5, 6, 7, 8, 9, 10, 11, 12, 13, 14, 15, 16]. Similar to the Fermi Hubbard model, the Bose-Hubbard model can be used to explore the effects of the strong correlations. Unlike the fermi system, there is no "sign problem" in bosonic case, so the Quantum Monte Carlo (QMC) simulations can be successfully performed. Many interesting results have been found in these models, such as supersolid phase, valence-bond-solid phase and striped phase.

In the past several years, although the extended Bose-Hubbard model on two-dimensional square lattice [5, 6] and triangular lattice [7, 8, 9, 10, 11] has been studied extensively using QMC methods, another common lattice, honeycomb lattice has rarely been studied by QMC. In [13], by using a dual vortex method (DVM), one of the authors studied phases such as superfluid, solid, supersolid and quantum phase transitions in an extended boson Hubbard model such as Eqn.1 slightly away from half filling on bipartite lattices such as honeycomb and square lattice. He found that in the insulating side, different kinds of supersolids are generic possible states slightly away from half filling and also proposed a new kind of supersolid: valence bond supersolid which maybe stabilized by possible ring exchange interactions. He showed that the quantum phase transitions from solids to supersolids driven by a chemical potential are in the same universality class as that from a Mott insulator to a superfluid, therefore have exact exponents  $z = 2, \nu = 1/2, \eta = 0$ . For example, near the solid to the supersolid transition,

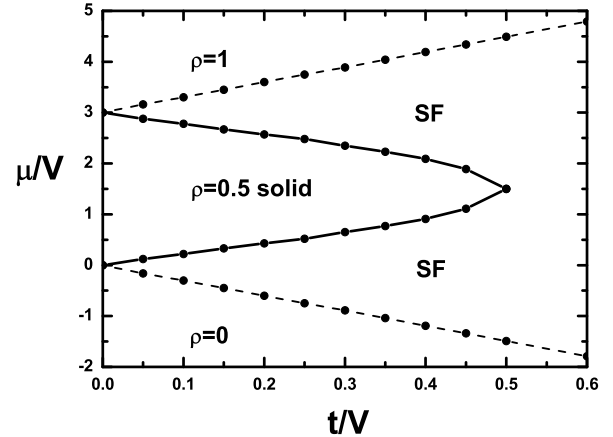


FIG. 1: The ground-state phase diagram for 2D hard-core Bose-Hubbard model on the honeycomb lattice in the grand canonical ensemble obtained from quantum Monte Carlo simulation. SF: superfluid phase. The solid line is first order transition, while the dashed line is second order.

the superfluid density inside the supersolid phase should scale as  $\rho_s \sim |\rho - 1/2|^{(d+z-2)\nu} = |\rho - 1/2| = \delta f$  with possible logarithmic corrections. Comparisons with previous quantum Monte-Carlo (QMC) simulations on a square lattice are made.

The DVM is a magnetic space group (MSG) symmetry-based approach which can be used to classify some important phases and phase transitions. But the question if a particular phase will appear or not as a

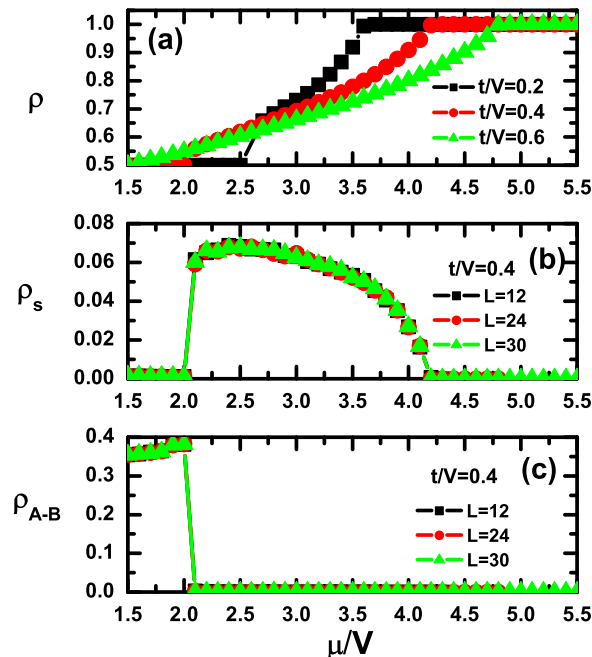


FIG. 2: (color online). (a) The boson density  $\rho$  as a function of chemical potential  $\mu$  for  $\beta = 100V$  and  $L = 24$ . (b) and (c) are superfluid density  $\rho_s$  and  $\rho_{A-B}$  as functions of  $\mu$  for  $t/V = 0.4$ ,  $\beta = 100V$ , and  $L = 12, 24, 30$  respectively.

ground state can not be addressed in this approach, because it depends on the specific values of all the possible parameters in the EBHM in Eqn.1. So a microscopic approach such as Quantum Monte-Carlo (QMC) is needed to compare with the DVM. The DVM can guide the QMC to search for particular phases and phase transitions in a specific model. Finite size scalings in QMC can be used to confirm the universality class discovered by the dual approach. So far, there is no QMC simulations on a honeycomb lattice. In this paper, we study the extended Bose-Hubbard model on a honeycomb lattice by QMC simulations and also compare with the results achieved in [13] by the DVM. We find that the ground-state phase diagram is qualitatively similar to the one obtained on square lattice. In the hard-core limit, the supersolid state is unstable towards the phase separation. The transition between  $\rho = 1/2$  solid and the superfluid is the first order one. In the soft-core case, due to the presence of the multiple occupation, a stable particle doped supersolid (SS-p) phase emerges when bosons are doped into  $\rho = 1/2$  solid (i.e., fillings  $\rho > 1/2$ ). We find the solid at  $\rho = 1/2$  to the SS-p at  $\rho > 1/2$  is a second order transition, the superfluid density inside the SS-p scales as  $\rho_s \sim \rho - 1/2$  which is consistent with the result achieved in [13] by the DVM. Very precise finite size scalings by QMC [17] are under-

way to test the exact exponents  $z = 2, \nu = 1/2, \eta = 0$ . However, a hole doped supersolid phase remains unstable to phase separation when vacancies are doped into  $\rho = 1/2$  solid (i.e., fillings  $\rho < 1/2$ ). We also calculate the critical exponents of the transition between  $\rho = 1/2$  solid and superfluid at the Heisenberg point. We find the dynamical critical exponent  $z$  and the correlation length exponent  $\nu$  are  $z = 0.15$  and  $\nu = 0.38$ . The dynamical critical exponent we have obtained is smaller than it was previously obtained [18]. We speculate that  $z$  will approach zero as the size of the simulated system goes to infinity, so the the SF to the solid transition at the Heisenberg point remains first order.

The extended Bose-Hubbard model we study can be written as:

$$H = -t \sum_{\langle ij \rangle} (a_i^\dagger a_j + a_j^\dagger a_i) + \frac{U}{2} \sum_i n_i (n_i - 1) + V \sum_{\langle ij \rangle} n_i n_j - \mu \sum_i n_i \quad (1)$$

where  $a_i^\dagger (a_i)$  is the creation (annihilation) operator of the bosonic atom at site  $i$ ;  $n_i = a_i^\dagger a_i$  is the occupation number and  $\mu$  is the chemical potential.  $\langle ij \rangle$  runs over nearest neighbors.  $U$  and  $V$  represent the on-site and nearest-neighbor repulsive interaction, respectively. When  $U/t \rightarrow \infty$ , the Hamiltonian reduces to the hard-core one with no multiple occupation. The method we employ is the stochastic series expansion Quantum Monte Carlo (QMC) method with directed loop (SSE) [19].

In order to characterize different phases, usually one studies the static structure factor  $S(Q)$  and superfluid density  $\rho_s$  [20],

$$S(Q) = \frac{1}{N} \sum_{ij} e^{iQ \cdot (r_i - r_j)} \langle n_i n_j \rangle, \quad \rho_s = \frac{\langle W^2 \rangle}{4\beta t}, \quad (2)$$

where  $W$  is the winding number fluctuation of the bosonic lines,  $\beta$  is the inverse temperature, and  $N = 2 \times L \times L$  is the lattice size. In a honeycomb lattice,  $S(Q = (4\pi/3, 0))$  is always nonzero when  $\rho > 0$ , because  $Q = (4\pi/3, 0)$  is not only the wave vector for the solid phase but also the reciprocal vector on a honeycomb lattice. So it can not be used to characterize the solid order on a honeycomb lattice. Here we use the density difference between the two sublattice,  $\rho_{A-B}$ , to characterize the solid order for a honeycomb lattice,

$$\rho_{A-B} = |\rho_A - \rho_B|, \quad (3)$$

where  $\rho_A$  and  $\rho_B$  are the boson density for  $A$  and  $B$  sublattice respectively. The two parameters  $\rho_s$  and  $\rho_{A-B}$  can characterize different phases in the system: a solid phase is characterized by  $\rho_{A-B} \neq 0$  and  $\rho_s = 0$ ; a SF

phase by  $\rho_{A-B} = 0$  and  $\rho_s \neq 0$ ; a SS phase by both  $\rho_{A-B} \neq 0$  and  $\rho_s \neq 0$ . Different solid phases can be categorized by different values of  $\rho_{A-B}$ .

We first consider the hard-core limit, which is relatively simple. The phase diagram is presented in Fig. 1. This phase diagram can be qualitatively explained by strong-coupling arguments. For  $\mu < -3t$ , the system is empty, while for  $\mu > 3(t+V)$ , it is a Mott insulator with one boson per site. At large values of  $t/V$ , the system exhibits a superfluid phase. A solid phase with  $\rho = 1/2$  emerges in small values of  $t/V$ . At  $\mu/V = 1.5$ , the critical point between superfluid phase and  $\rho = 1/2$  solid is at  $(t/V)_C = 0.5$ . This point  $(t/V, \mu/V) = (0.5, 1.5)$  is the Heisenberg point.

When bosons (holes) are doped into the  $\rho = 1/2$  solid, the domain wall proliferation mechanism, i.e., the additional bosons (holes) can hop freely across the domain wall, gain the kinetic energy linearly in  $t$ , hence excludes the stable supersolid state [6, 7]. The transition from the  $\rho = 1/2$  solid to the superfluid is the first order one (see Fig. 2(a)). The phase diagram is qualitatively similar to the one obtained for a square lattice. This is not surprising since both the square lattice and the honeycomb lattice are bipartite lattices. However, the phase boundary is quantitatively different. This comes from the different coordinate number of two lattices, i.e.,  $q = 3$  for the honeycomb lattice and  $q = 4$  for the square lattice. Fig. 2 (a) shows the density  $\rho$  as a function of chemical potential  $\mu$ . For small values of  $t/V$  (say  $t/V = 0.2, 0.4$ ), there is a jump from  $\rho = 1/2$  to  $\rho > 1/2$ , which indicates a first-order transition. In the grand canonical ensemble, a jump in  $\rho$  is the token of a PS region. Fig. 2 (b) and (c) are the superfluid  $\rho_s$  and  $\rho_{A-B}$  as functions of  $\mu$  for  $t/V = 0.4$ . For  $\mu/V \leq 2$ ,  $\rho_s = 0$  while  $\rho_{A-B} \neq 0$ , the ground-state is the  $\rho = 1/2$  solid; for  $2 \leq \mu/V \leq 4.2$ ,  $\rho_s \neq 0$  while  $\rho_{A-B} = 0$ , the ground-state is a superfluid phase; at the critical point  $\mu_C/V = 2$ , both  $\rho_s$  and  $\rho_{A-B}$  have a jump, indicating the first order transition; for  $\mu/V > 4.2$ , both  $\rho_s = 0$  and  $\rho_{A-B} = 0$  with  $\rho = 1$ , the ground-state is a Mott insulator. There is no region for both  $\rho_s$  and  $\rho_{A-B}$  nonzero, i.e., no stable supersolid state.

In the above we have found that there is no stable supersolid phase in the hard-core Bose-Hubbard model in a honeycomb lattice, similar to a square lattice. It was found that by softening the onsite interaction  $U$ , i.e., in the soft-core case, a stable supersolid state emerges on the 2D square lattice [6]. Motivated by this, we next consider the soft-core case on the 2D honeycomb lattice. Hereafter we fix  $U = 15t$  and  $\beta = 2L$  in our calculations.

Fig. 3 shows the phase diagram for the soft-core honeycomb lattice at  $U = 15t$ . The phase diagram is not symmetric respect to  $\mu/V = 1.5$  because finite  $U$  breaks the particle-hole symmetry. Besides the  $\rho = 0$  solid,  $\rho = 1/2$  solid (we named it CDW I here) and the Mott insulator ( $U > 3V$ ) which already emerge in the hard-core case, an-

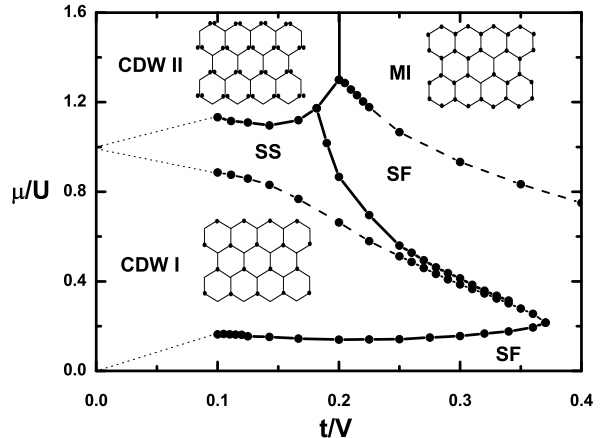


FIG. 3: The ground-state phase diagram for 2D soft-core Bose-Hubbard model on the honeycomb lattice obtained from quantum Monte carlo simulation. SF: superfluid phase; SS: supersolid phase; PS: phase separation; CDW I:  $\rho = 1/2$  solid with one sublattice occupied and one boson per site; CDW II:  $\rho = 1$  solid with one sublattice occupied and two bosons per site; MI: Mott insulator phase with one boson per site. The solid line is first order. The dashed line is second order.

other  $\rho = 1$  solid ( $U < 3V$ ) with one sublattice occupied by two bosons per site emerges. We call this phase CDW II. A supersolid state emerges when atoms are doped into the  $\rho = 1/2$  solid, while the supersolid phase is unstable towards the phase separation when holes are doped into the  $\rho = 1/2$  solid due to the domain wall mechanism just like what happens in the hard-core case. The main reason for the emergence of the CDW II and supersolid state, is the possible multiple occupation in the soft-core case. When bosons are doped into the  $\rho = 1/2$  solid, the additional bosons can occupy either occupied or unoccupied sites. When  $|3V - U| \sim t$ , the doped bosons can form a superfluid on top of the  $\rho = 1/2$  solid background, this phase is a supersolid phase. Similar results have been found in the 2D soft-core square lattice [6], 2D triangular lattice [11] and 1D chain [21].

Fig. 4 (a) is the plot of  $\rho$  v.s.  $\mu$  for  $U = 15t$ . For a density  $\rho$  just less than  $1/2$ , there are jumps in  $\rho - \mu$  plot, which indicate the transition is a first order transition and the ground-state is a phase separation. This also indicates that the possible hole-doped supersolid (SS-h) phase is unstable against the phase separation. The jump also emerges in the fillings just less than 1 for large  $V$  (say  $V = 6t$ ). This indicates that the CDW II to the supersolid transition is 1st order. Fig. 4 (b) and (c) shows the finite size scaling of superfluid density  $\rho_s$  and the diagonal long range order  $\rho_{A-B}$  as functions of  $\rho$  for  $V = 4t$  and  $6t$ , respectively. From these figures, we can identify the regions of superfluid with  $\rho_s \neq 0$ ;  $\rho = 1/2$

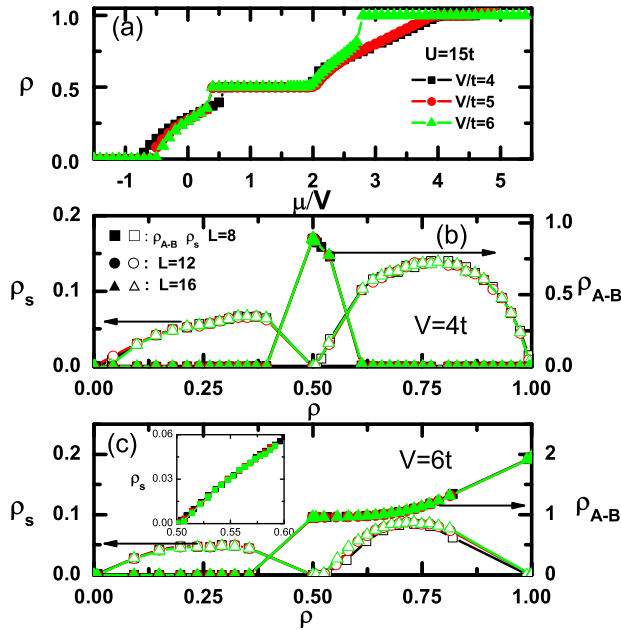


FIG. 4: (color online). (a): The boson density  $\rho$  as a function of  $\mu$  for  $V = 4t, 5t, 6t$  at  $U = 15t$  and  $\beta = 2L$  for soft-core case. (b) (c): The finite size scaling of superfluid density  $\rho_s$  and diagonal long range order  $\rho_{A-B}$  as a function of  $\rho$  for  $V = 4t, 6t$  respectively for soft-core case.

solid with  $\rho_{A-B} \neq 0$ ; supersolid with both  $\rho_s \neq 0$  and  $\rho_{A-B} \neq 0$ ; phase separation with  $\rho_s$  and  $\rho_{A-B}$  showing discontinuity. In the inset of Fig.4(c) we also find that near  $\rho = 1/2$ , superfluid density scales as  $\rho_s \sim (\rho - 1/2)^1$ . This is consistent with the superfluid scaling derived by the DVM in [13].  $\rho_{A-B}$  also changes smoothly across the the CDW-I to the SS-p transition. So the SS-p has the same diagonal order as the CDW-I. These facts conclude that the transition from CDW I to SS-p is of second order. In fact, as shown by the DVM, the transition is in the same universality class as that from a Mott insulator to a superfluid, therefore has exact exponents  $z = 2, \nu = 1/2, \eta = 0$ . Very precise finite size scalings by QMC [17] are underway to test the universality class [17]. Possible ring exchange terms will also be added in [17] to test the possible valence bond supersolid proposed by the DVM in [13].

As shown by the DVM in [13], due to the change of saddle point structure of the dual gauge field on the CDW-I and SF, the SF to the CDW-I is a first order transition. The SF to the SS-p is also first order. Fig.1 shows that the SF to the SS-p is indeed first order. However, in Fig.3, our QMC data in Fig.3 can not determine if the SF to the SS-p is first order or second order. More precise QMC such as double-peak histogram maybe needed

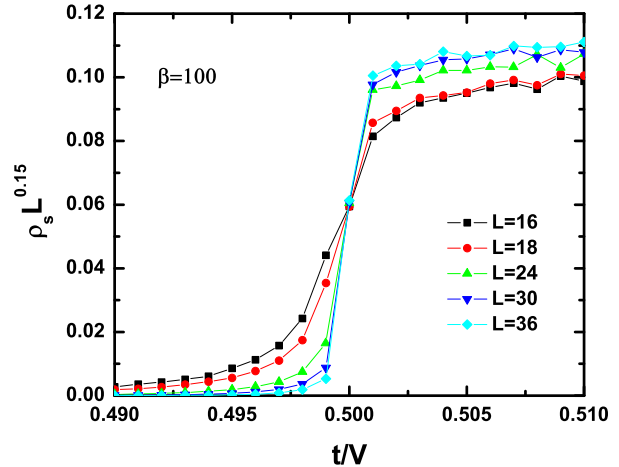


FIG. 5: (color online).  $\rho_s$  as a function of  $t/V$  for  $L = 16, 18, 24, 30, 36$  for  $\beta = 100V$  at  $\mu/V = 1.5$ . The intersection at  $t/V = 0.5$  is the critical point.

to determine the nature of the SF to the SS-p transition.

For the hard core case, at  $t/V = 0.5$ , corresponding to the isotropic Heisenberg point of the spin-1/2 quantum antiferromagnetic model, the half filled solid melts to superfluid. The critical behavior of this Heisenberg point is controversial. By assuming a second order transition, Hébert *et.al.* [18] found rather exotic critical exponents,  $z = 0.25$  and  $\nu = 0.36$ . However, by studying the XXZ model crossing the isotropic point, Sandvik and Melko point out that the critical exponent  $z$  will become zero in the thermodynamic limit [22].

In the below, by taking the same strategy as Hébert *et.al.* [18], e.g. assuming it is a second order quantum phase transition crossing the Heisenberg point, we also calculate the critical exponents for the 2D hard-core boson model on the honeycomb lattice at the Heisenberg point. The finite size scaling function of superfluid density is assumed to have the following form [2]:

$$\rho_s = \frac{1}{L^z} F((t/V - (t/V)_C) L^{1/\nu}, \beta/L^z), \quad (4)$$

where  $z$  is the dynamical critical exponent,  $\nu$  is the correlation length exponent, and  $F$  is the corresponding scaling function. Note that the finite size scaling function  $F$  does not only depend on the scaled distance to the critical point  $((t/V - (t/V)_C) L^{1/\nu})$ , but also on the ratio of the inverse temperature and the lattice size  $(\beta/L^z)$ . To obtain the critical exponents, one should simulate several sets of lattice sizes ( $L$ ), each set with different values of  $z$ . Here we follow the procedure of Ref. [18] for the square lattice, e.g. we fix a large enough  $\beta$  so that we can assume the second term of  $F$  is a constant as  $L$  is varied. With this choice,  $\rho_s L^z$  must be independent of  $L$  at the critical

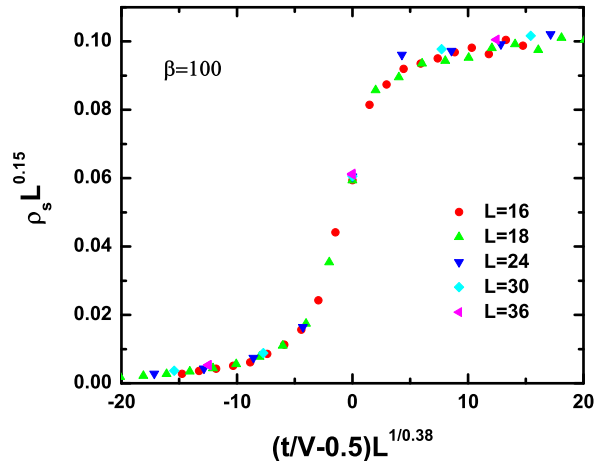


FIG. 6: (color online). Data collapse of the superfluid density  $\rho_s$  for  $\beta = 100V$  at  $\mu/V = 1.5$ . This yields the critical exponents  $z = 0.15$  and  $\nu = 0.38$ .

point ( $t/V = 0.5$ ). We calculate  $\beta = 20, 40, 60, 80$ , and  $100$  and find the results depend little on temperature. In the below, we present results only of  $\beta = 100$ .

First we simulate on smaller lattices  $L = 6, 8, 10, 12$  and we obtain the same exponents as Ref. [18] (not show here). Then we simulate on larger lattices, e.g.  $L = 16, 18, 24, 30, 36$ . The best intersection we found is at  $z = 0.15$  (Fig. 5). Replotting this figure by the scaled variable  $(t/V - 0.5)L^{1/\nu}$ , the best data collapse we found is at  $\nu = 0.38$  (see fig. 6).

The dynamical exponent we have obtained on larger lattices is smaller than that on smaller lattices. We speculate that it will approach zero in the thermodynamic limit, so the transition is first order, though it maybe very weak. This scenario is consistent with Sandvik's conclusion on XXZ model on square lattice [22].

In conclusion, we have studied the extended Bose-Hubbard model on a two-dimensional honeycomb lattice by using the quantum Monte Carlo simulation with the stochastic series expansion (SSE). We present the results both in the hard-core and soft-core case. We find that for the hard-core case, the supersolid state is unstable towards the phase separation due to the domain wall proliferation mechanism. The transition between  $\rho = 1/2$  solid and the superfluid is the first order one. For the soft-core case, due to the presence of the multiple occupation, a stable particle induced supersolid (SS-p) phase emerges when atoms are doped into  $\rho = 1/2$  solid (i.e., fillings  $\rho > 1/2$ ), while for fillings  $\rho < 1/2$ , the possible hole induced supersolid (SS-h) phase is unstable towards phase separation. The results are qualitatively similar to the one obtained for a square lattice. We found the CDW-I to the SS-p transition is second order with the super-

fluid density inside the SS-p scaling as  $\rho_s \sim \rho - 1/2$ , the SS-p has the same diagonal order as the CDW-I (Fig.3). However, the SS-p to the CDW-II transition is first order with jumps in both  $\rho_s$  and  $\rho_{A-B}$ . All these results are consistent with those achieved by the DVM in [13]. We also calculate the critical exponents of the transition between  $\rho = 1/2$  solid and the superfluid at Heisenberg point. The dynamical critical exponent  $z$  and the correlation length exponent  $\nu$  we find is  $z = 0.15$  and  $\nu = 0.38$ . However, we expect that  $z$  is size dependent and approaches zero in thermodynamic limit. This fact indicates that the solid to the SF transition is still 1st order even at the Heisenberg point.

*Note added.* Recently, we become aware of a similar work [23], where similar results are obtained.

Y.C.Wen and J.Y.Gan would like to thank S. M. Li, X. C. Lu, S. J. Qin and Z. B. Su for helpful discussion. J. Ye thanks Prof. Quangshan Tian for hospitality during his visit at Beijing university. This work was supported in part by Chinese National Natural Science Foundation and China Postdoctoral Science Foundation No.20060390079. S. J. Yang is supported by NSFC under grant No. 10574012. The simulations were performed on the HP-SC45 Sigma-X parallel computer of ITP and ICTS, CAS .

- 
- [1] I. Bloch, Physics world, **17**, 25-29 (2004); I. Bloch, Nature Physics **1**, 23-30 (2005).
  - [2] M. P. A. Fisher, P. B. Weichman, G. Grinstein, and D. S. Fisher, Phys. Rev. B **40**, 546 (1989).
  - [3] D. Jaksch, C. Bruder, J. I. Cirac, C. W. Gardiner, and P. Zoller, Phys. Rev. Lett. **81**, 3108 (1998).
  - [4] G. G. Batrouni, F. Hebert, and R. T. Scalettar, Phys. Rev. Lett. **97**, 087209 (2006).
  - [5] G. G. Batrouni and R. T. Scalettar, Phys. Rev. Lett. **84**, 1599 (2000).
  - [6] P. Sengupta, L. P. Pryadko, F. Alet, M. Troyer, and G. Schmid, Phys. Rev. Lett. **94**, 207202 (2005).
  - [7] S. Wessel and M. Troyer, Phys. Rev. Lett. **95**, 127205 (2005).
  - [8] D. Heidarian and K. Damle, Phys. Rev. Lett. **95**, 127206 (2005).
  - [9] R. G. Melko, A. Paramekanti, A. A. Burkov, A. Vishwanath, D. N. Sheng and L. Balents, Phys. Rev. Lett. **95**, 127207 (2005).
  - [10] M. Boninsegni and N. Prokof'ev, Phys. Rev. Lett. **95**, 237204 (2005).
  - [11] Jing Yu Gan, Yu Chuan Wen and Yue Yu, Phys. Rev. B, **75**, 094501 (2007).
  - [12] Longhua Jiang and Jinwu Ye, J. Phys. Condens. Matter **18**, 6907-6922 (2006).
  - [13] Jinwu Ye, cond-mat/0503113.
  - [14] R. G. Melko, A. Del Maestro, and A. A. Burkov, Phys. Rev. B **74**, 214517 (2006) .
  - [15] S. V. Isakov, S. Wessel, R. G. Melko, K. Sengupta, and Y. B. Kim, Phys. Rev. Lett. **97**, 147202 (2006).
  - [16] Jinwu Ye, cond-mat/0612009.

- [17] Jing Yu Gan, Yu Chuan Wen, Jinwu Ye, Yue Yu *et. al.*, unpublished.
- [18] F. Hébert, G. G. Batrouni, R. T. Scalettar, G. Schmid, M. Troyer and A. Dorneich, Phys. Rev. B **65**, 014513 (2001).
- [19] O. F. Syljuåsen, and A. W. Sandvik, Phys. Rev. E **66**, 046701 (2002).
- [20] E. L. Pollock and D. M. Ceperley, Phys. Rev. B **36**, 8343 (1987).
- [21] G. G. Batrouni, F. Hébert, and R. T. Scalettar, Phys. Rev. Lett. **97**, 087209 (2006).
- [22] A. W. Sandvik, and R. G. Melko, cond-mat/0604451.
- [23] S. Wessel, cond-mat/0701337.